LANGMUIR

pubs.acs.org/Langmuir Article

Sticking Effect of a Tackifier on the Fibrillation of Acrylic Pressure-Sensitive Adhesives

Kosuke Takahashi,* Futoshi Yanai, Kazuaki Inaba, Kikuo Kishimoto, Yuichi Kozone, and Toshio Sugizaki

Cite This: https://doi.org/10.1021/acs.langmuir.1c01381 Read Online

ACCESS | Metrics & More | Article Recommendations | Supporting Information

ABSTRACT: In this study, the effect of a tackifier on the viscoelastic and adhesion properties of acrylic pressure-sensitive adhesives (PSAs) was investigated. The intermediate products in the process of PSA synthesis, including an acrylate-based copolymer solution, a cross-linked copolymer, and the final product with a tackifier, were prepared and characterized using dynamic mechanical analysis (DMA). A significant increase in storage and loss moduli at high angular velocities was observed for the final product with the tackifier. The adhesion forces of the copolymer solution and the cross-linked copolymer measured by atomic force microscopy (AFM) were found to be almost independent of the release velocity, whereas that of the final product with the tackifier significantly increased at higher release velocities because of viscoelastic effects. Their fibrillations during the release process were also visualized using a charge-coupled device (CCD) camera installed on the cantilever holder. Although the contact area of the copolymer solution and the cross-linked copolymer with the probe surface decreased until detachment, the final product with the tackifier remained constant, with necking just below the probe surface. The increased storage and loss moduli were considered to resist the shrinkage of the contact area because the contact outline was subject to high shearing deformation, which led to localized high strain rates. Overall, the crucial role of the tackifier in maintaining the contact area for sufficient elongation during fibrillation was established.

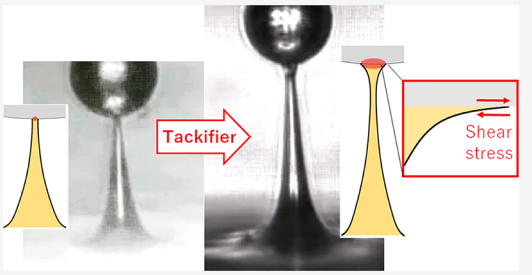

INTRODUCTION

Pressure-sensitive adhesives (PSAs) can be instantly applied to and cleanly separated from various surfaces via slight pressure application.[1] The unique nonreactive adhesion of PSAs makes them compatible to the human skin, and therefore, PSAs are extensively used in the medical field as surgical tapes and compresses.[2] Furthermore, these surgical tapes can be applied to both outer skin and internal organs when modified to adhere to wet surfaces.[3] In addition, the excellent flexibility upon bonding is useful in electronics requiring buffering of thermally induced stresses, which cannot be achieved using structural adhesives.[1,4] Reliable adhesion under variable loading conditions is becoming the driving force for an increasing usage of PSAs in flexible electric displays.[5] Although these unique properties of PSAs have enabled their utilization in a variety of applications, a deeper understanding of the adhesion mechanism is still indispensable for further development of PSAs.

The adhesion performance of PSAs has been extensively investigated based on various parameters such as adherent surface roughness,[6,7] contact time,[8−10] and release rate.[11−14] In general, a PSA material must be sufficiently fluid to penetrate the surface roughness of a substrate and generate significant van der Waals forces. Simultaneously, the material must exhibit sufficient stiffness to resist deformation by peeling. Both characteristics are achieved by tuning the viscoelastic properties of the PSA, which in turn can be controlled by selecting appropriate molecules and using polymerization techniques.[15−23] However, for rubber-based PSAs, stickiness can only be achieved by adding tackifiers.[24,25] Tackifiers are chemical compounds with a low molecular weight and high glass-transition temperature, which imparts stickiness to the rubbery polymers.[26] Although acrylic PSAs with suitable viscoelasticity are already sticky, their adhesion performance can be significantly improved by adding a tackifier.[27,28] However, the general mechanism for this improved adhesion performance has not been fully understood as the production of PSAs with added tackifiers is typically based on empirical data.

In our previous studies, the adhesion performance of PSAs was studied using a probe tack test.[29−31] The test enables accurate measurement of the adhesion force from probe contact to release with direct observation of the contact

Received: May 24, 2021

area.[32−35] Separation force initially increases linearly, followed by a sharp decrease because of cavity growth or fingering near the probe interface, and then gradually increases again because of fibrillation until complete separation is achieved.[36,37] The maximum adhesion stress of industrial PSAs during the release process is typically determined based on cavity growth[38−40] and can be successfully characterized using a criterion proposed in our previous work.[30] The fibrillation process was also characterized by comparing our probe tack tests with different probe scales using a millimeter-scale glass sphere and an atomic force microscopy (AFM) cantilever.[31] In contrast to the macroscopic probe tack test, the tiny contact area of the cantilever in AFM did not cause cavity growth, which was useful to focus on the detachment behaviors of PSAs from a probe, followed by fibrillation.

This study aimed at revealing the effects of tackifier addition on the viscoelasticity of a PSA material utilizing our established experimental schemes for evaluating the adhesion performance. An acrylic PSA with a tackifier and its intermediate products, including the copolymer solution and the cross-linked copolymer were synthesized. The effects of each process on the adhesion performance of the samples were investigated. The viscoelastic properties were analyzed using dynamic mechanical analysis (DMA), and the adhesion performances were examined using the probe tack test with an AFM cantilever. The adhesion forces during the release process were measured with in situ observations. A test based on the glass sphere attached to the tip of the AFM cantilever was also conducted to observe the detachment behaviors more clearly and examine the effect of the probe shape. The change in the detachment behavior because of the tackifier was carefully observed and correlated to the viscoelastic properties to explain the mechanism of improved adhesion performance.

EXPERIMENTAL SECTION

Sample Preparation and Characterization. The intermediate products in the process of PSA synthesis, including acrylic-based copolymer solution (CS), cross-linked copolymer (CL), and the final product of the CL with a tackifier (PSA) were prepared as samples. First, purified butyl acrylate, methyl methacrylate, and 4-hydroxybutyl acrylate were stirred with an initiator, azobisisobutyronitrile, in ethyl acetate under a nitrogen atmosphere at 60 °C for 8 h to obtain CS samples. The chemical structure and the degree of polymerization are provided in the Supporting Information. The molecular weight and polydispersity index of the copolymer were 600,000 Da and 5.9, respectively. The solution was adjusted to 30% nonvolatile components in the flask. Next, an *m*-xylylene diisocyanate-derived cross-linker was added to the solution to make it up to a concentration of 35%. The mixture was then dissolved in ethyl acetate and coated on polyester films, followed by drying at 100 °C to obtain CL samples. For PSA samples, an extra-hydrogenated rosin ester (softening point: 100 °C) was also mixed at 20% relative concentration to the copolymer prior to the coating. The main component of the extra-hydrogenated rosin ester was obtained from abietic acid, whose conjugated double bond was hydrogenated. The spatial distribution of the tackifier in a similar acrylic-based copolymer was confirmed to be uniform and in the order of a nanometer scale, according to the AFM analysis.[41] Although aromatic tackifiers are generically hard to dissolve in the acrylate copolymer, both can be dissolved in the ethyl acetate solution. A fine dispersion of the tackifier through the drying process was considered to be obtained by the miscibility of the rosin ester resin with the elastomer part of the copolymer in the analyzed composition range.

DMA was conducted using a rheometer (Physica MCR300, Anton Paar) with parallel circular plates (diameter = 8 mm) in shear mode. The samples were laminated to a thickness of 0.8 mm. First, the angular velocity was varied from 1 to 100 rad/s at temperatures −20, 0, 23, and 60 °C to obtain master curves for the storage (G') and loss (G'') moduli. The shift factors were selected to ensure that the storage modulus measurements at various temperatures could be plotted smoothly with respect to the measurement at room temperature (23 °C). Next, a fixed frequency (10 Hz) and strain (5%) were applied, while the temperature was gradually increased from −20 to 80 °C to obtain the loss tangent (tan δ) maxima. The CS sample was not analyzed as it was difficult to maintain the sample, particularly at high temperatures.

Force Curve Measurements with In Situ Observation of Fibrillation. The adhesion performance of the samples was evaluated based on the observations of the elongation using AFM in tapping mode (Nanowizard II, JPK). The dimensions of the AFM cantilever (All-In-One-Al-D, Budget Sensors) are shown in Figure 1a. The force

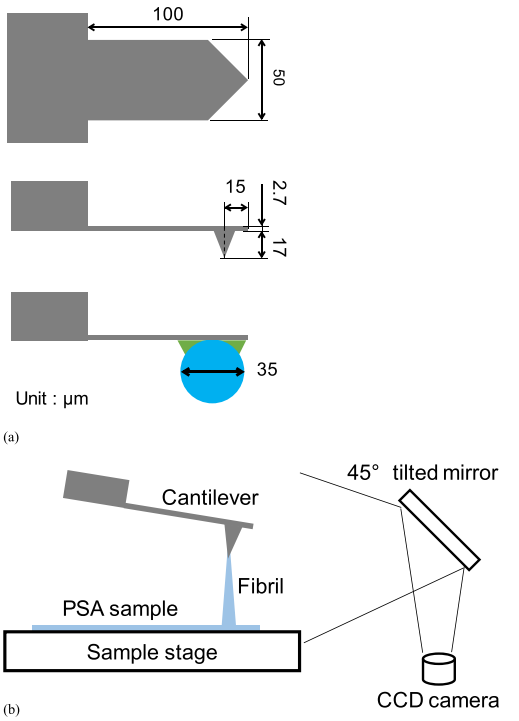

Figure 1. Dimensions of (a) the AFM cantilever (above) and glass bead attached to the cantilever used for the force measurement (below), and (b) schematic illustration of the set-up for in situ observation using a CCD camera.

constant of the cantilever was 40 N/m. The cantilever had a 30 nm thick aluminum reflective coating on the detector side; it was fixed on a holder with a mirror tilted at 45° relative to the charge-coupled device (CCD) camera below (SideView CantileverHolder, JPK). Prior to each test, the cantilever was blown to remove electrostatic effects using a bench-top ionizer (ENZR-B, Misumi Corp.) and carefully cleaned using an ultraviolet (UV)−ozone cleaner (TC-003, BioForce Nanosciences).

The CS, CL, and PSA samples were each cast on a release liner, dried at 90 °C for 1 min, and spread on glass plates at thicknesses of 5, 15, 25, and 50 μm using a film applicator. The samples were stored at room temperature prior to AFM analyses. The AFM cantilever was inserted into the sample at an approaching velocity of 0.2 μm/s until the compressive force reached 1000 nN. Subsequently, the AFM cantilever was retracted to detach from the sample surface at either 0.05, 0.2, or 1.0 μm/s. The force and displacement of the cantilever were measured along with the observation using the CCD camera from the initial contact until detachment. Our previous study confirmed the reproducible force curves using the same PSA sample, indicating that the spatial distribution of the tackifier was finer than the contact area of the AFM cantilever.

https://doi.org/10.1021/acs.langmuir.1c01381
Langmuir XXXX, XXX, XXX−XXX

An additional experiment was conducted using a glass sphere (diameter = 35 μm) attached to the tip of the AFM cantilever. This glass sphere probe was prepared to increase the contact area for capturing much clearer images using the CCD camera. Typically, the AFM cantilever was lowered into an uncured epoxy adhesive and then placed on the glass sphere until firmly fixed (Figure 1b). To avoid exceeding the load capacity of the AFM because of the increased contact area, the probe was retracted for detachment as soon as the compressive force reached 0.05 nN, which was the minimum contact force detectable by AFM. The approaching velocity toward the sample surface was controlled at the same 0.2 μm/s as in the experiment with an unmodified AFM cantilever.

RESULTS AND DISCUSSION

DMA. The master curves of G' and G'' are shown in Figure 2a,b, respectively. As expected, the CS sample exhibited the lowest G', particularly at lower angular velocities. However, it exhibited an increase in G' at higher velocities, which was also observed with the CL sample. The addition of a tackifier led to significant solidification at higher velocities, while promoting flexibility at low velocities (<0.1 rad/s). However, neither cross-linking nor tackifier addition had any effect on G' at an angular velocity in the order of 10 rad/s. Similarly, G'' of all three samples was almost identical, at an angular velocity ~1 rad/s. At higher velocities, all three samples continued to exhibit an increase in G''; however, the increase was more significant in the PSA sample.

Tan δ, as shown in Figure 2c, illustrates the significant effect of tackifier addition on the CL. At lower temperatures, which were equivalent to higher angular velocities, the tackifier significantly increased tan δ. Furthermore, the maxima increased by 1.5 times, and the corresponding temperature, which is an estimate of the glass-transition point, shifted from −20 to −5 °C. The increase in the maxima of tan δ and the glass-transition temperature, simultaneously given with the higher storage modulus, is the distinctive feature for the adhesion, which is sufficiently fluid for better contact but stiff for resisting deformation. These changes caused by tackifier addition have been reported in previous DMA analyses.[25,27]

A lower G' of the PSA sample at a sufficiently low velocity (<0.1 rad/s) implies that the dissolved tackifier molecules in the base copolymer imparted enough molecular mobility so that the copolymer could flow and wet the substrate effectively to form an adhesive bond.[42,43] At the same time, the spatially distributed tackifier agglomerates with a size on the order of several tens of nanometers are expected to render both the moduli more sensitive to the angular velocity. Although the detailed mechanism of how the morphology of the PSA affects the viscoelasticity remains to be verified in a future study, the significantly increased moduli at sufficiently high velocities (>100 rad/s) are expected to synergistically promote resistance against the rapid deformation of fibrillation during the release process.

AFM. *Effects of Cross-Linking and the Tackifier on Adhesion Force during the Release Process.* The relationship between the cantilever displacement and the adhesion force of the CS, CL, and PSA samples was studied using the AFM cantilever at various release velocities. The sample thickness was 15 μm. As shown in Figure 3a, the depths of the cantilever into the CS sample during compression varied slightly, whereas the maximum forces during release were similar, regardless of the release velocity. The maximum forces were always attained at a displacement of 0 μm, where the tip of the cantilever was positioned at the height of the sample surface. It could be

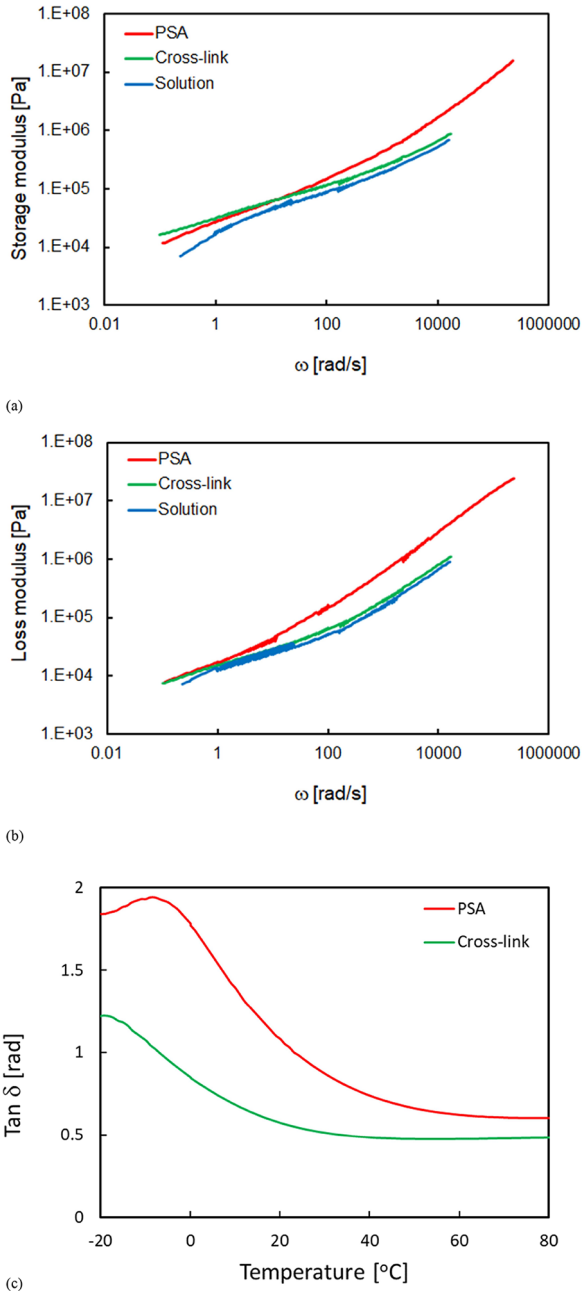

Figure 2. Master curve of the (a) storage modulus, (b) loss modulus, and (c) loss tangent at 10 Hz of the CS (solution), CL (cross-linked), and PSA.

stated that the CS sample rose to form a meniscus upon contact with the cantilever; however, it gradually receded because of the inability to sustain tension after the tip of the cantilever left the sample surface. The CL sample exhibited a continuous increase even after the tip of the cantilever left the sample surface, followed by a steeper increase in the adhesion force at a displacement of ~5 μm, as shown in Figure 3b. This corresponds to the typical behavior of the loosening of polymer chain entanglement at the beginning of the tension, followed by the stretching of polymer chains under further tension. It should be noted that a 20-fold increase in the release velocity from 0.05 to 1 μm/s did not have any effect on the elongation process, confirming the negligible viscoelastic effects in this range of release velocity. By contrast, the

https://doi.org/10.1021/acs.langmuir.1c01381
Langmuir XXXX, XXX, XXX−XXX

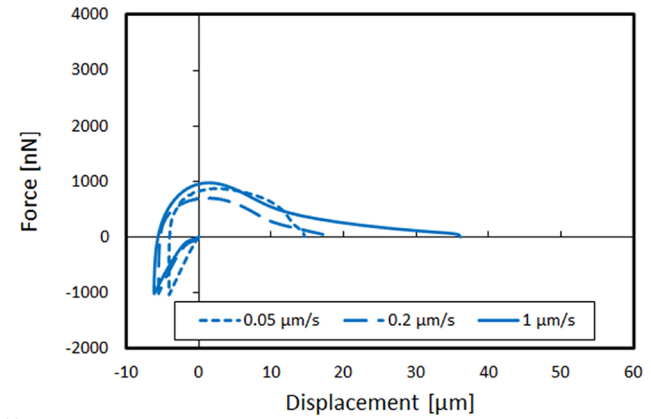

(a)

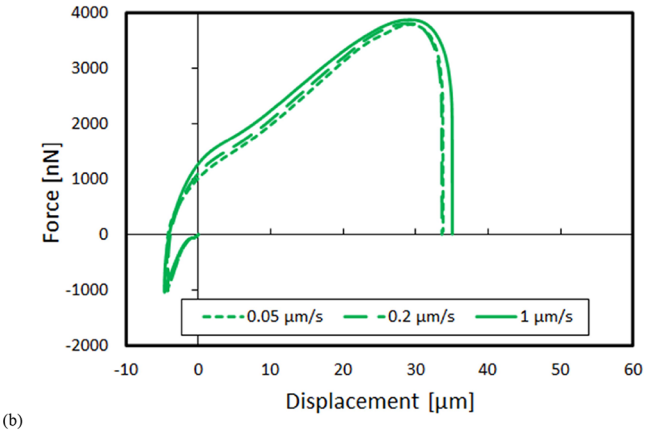

(b)

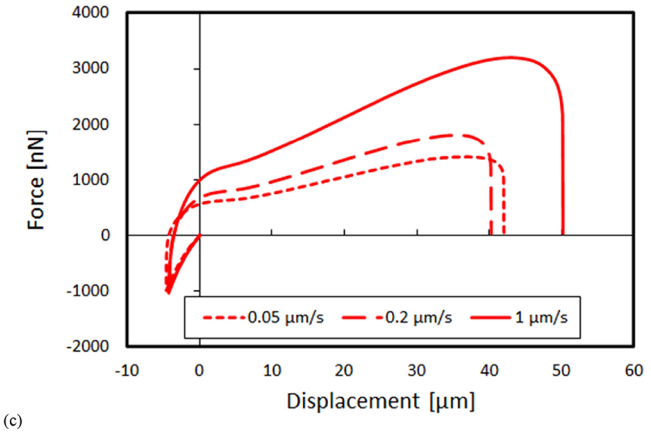

(c)

Figure 3. Relationship between adhesion force and elongation at various release velocities for the (a) CS, (b) CL, and (c) PSA (sample thickness = 15 μm).

addition of the tackifier resulted in a higher adhesion force with longer elongation at a higher release velocity (Figure 3c). The viscoelastic effect clearly appeared during the elongation process; thus, improved adhesion performance could be observed at higher release velocity.

To confirm the improvement of the adhesion force by the viscoelastic effect, the PSA sample was examined at a higher release velocity of up to 150 μm/s (Figure 4). The maximum adhesion force increased continuously and was proportional to the fourth root of the release velocity.[44] Hence, it was proved

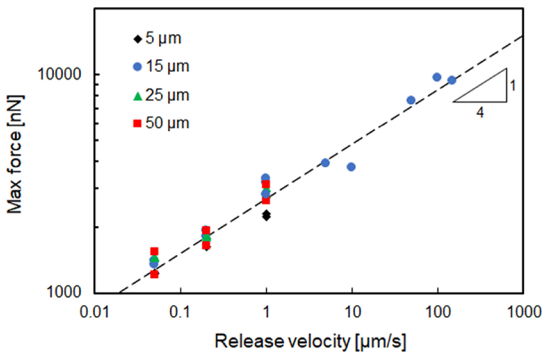

Figure 4. Relationship between release velocity and maximum adhesion force of the PSA sample.

that the adhesion strength can be improved at a sufficiently high release velocity by adding the tackifier. The effect of sample thickness was also investigated based on the samples of the final product with tackifiers of thicknesses 5, 25, and 50 μm. It was found that the maximum adhesion force that facilitated detachment from the cantilever was not affected by sample thickness, which is consistent with the findings of our previous work.[31]

In Situ Observation of Fibrillation with Force Measurements. The adhesion forces at a release velocity of 1 μm/s recorded for the three samples were compared (Figure 5a). As the adhesion forces until a displacement of 0 μm (i.e., the tip of the cantilever at the sample surface) were similar, neither cross-linking nor the tackifier affected the contact process in which the samples wetted the cantilever. The highest maximum adhesion force was observed with the CL sample, implying that the tackifier addition is not always effective. A sample without a tackifier may exhibit higher adhesion force, particularly at low release rates because it is less sensitive to the release velocity. However, tackifier addition significantly increased the displacement at the detachment, whereas the CS and the CL exhibited similar displacements despite differences in adhesion force.

The fibrillation during the release process was also compared based on the images captured using the CCD camera (Figure 5b,c,d). These images were captured at six different displacement positions, as marked in Figure 5a. No distinct differences were observed in the first two images of all three samples, which were acquired from compression to release through a displacement of 0 μm. According to the contact depth, approximately 5 μm, as shown in Figure 5a, the corresponding contact radius was estimated to be 1 μm, considering the shape of the cantilever. The red arrow in the second image in Figure 5d represents the predicted contact diameter of 2 μm. It looked slightly shorter than the tip of the cantilever, which indicates the formation of the meniscus upon contact with the sample. The third images were also similar despite significantly different adhesion forces, as noted in Figure 5a. The fourth image finally revealed the difference where a rapid shrinkage of the extracted volume was observed in the CS sample, leading to the formation of a thin stringlike structure, as visible in the fifth image. By contrast, CL and PSA samples exhibited a conical shape of fibrillation in their fourth image. As the elongation proceeded (fifth image), the PSA sample was highly stretched near the tip of the cantilever while the CL sample continued to exhibit a thick conical shape. Finally, all samples exhibited separation in proximity to the tip of the cantilever.

https://doi.org/10.1021/acs.langmuir.1c01381
Langmuir XXXX, XXX, XXX−XXX

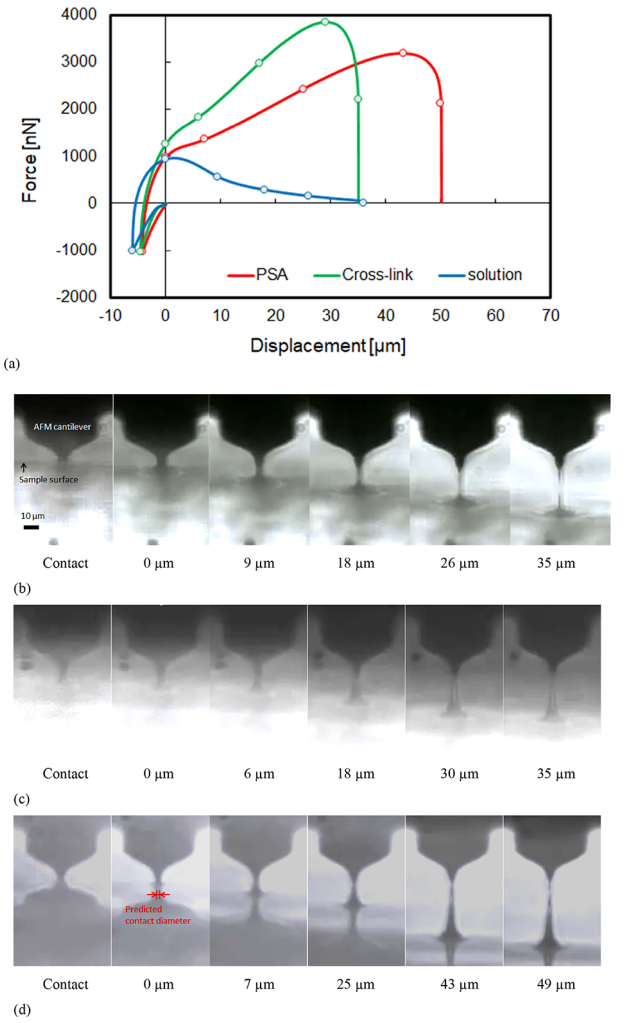

Figure 5. (a) Adhesion force using an AFM cantilever at a release velocity of 1 μm/s (sample thickness = 15 μm) and corresponding in situ observations of the (b) CS (solution), (c) CL (cross-linked), and (d) PSA.

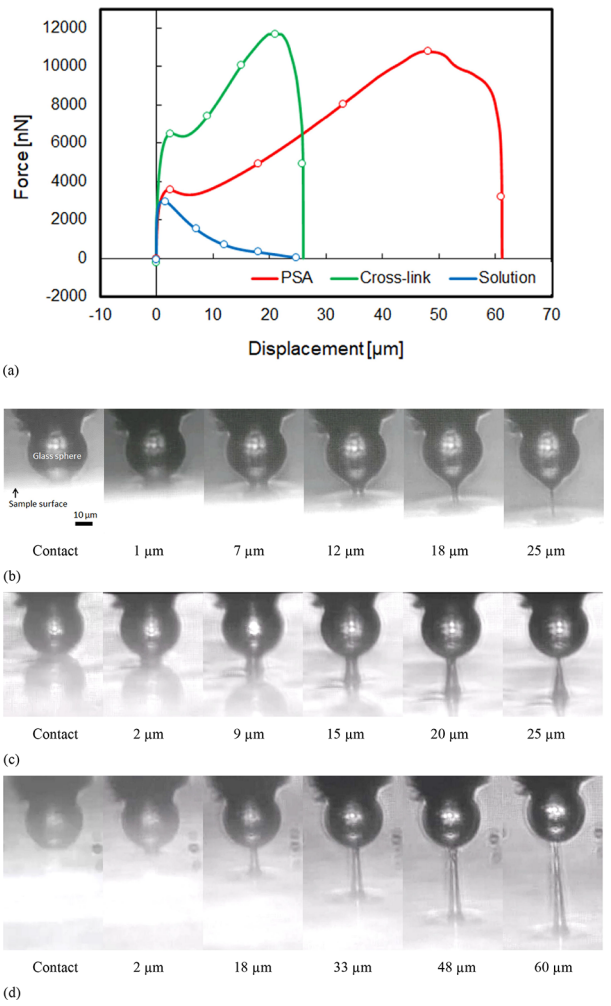

Figure 6. (a) Adhesion force using an AFM cantilever with an attached glass sphere at a release velocity of 1 μm/s (sample thickness = 15 μm) and corresponding in situ observations of the (b) CS (solution), (c) CL (cross-linked), and (d) PSA.

The aforementioned experiments were repeated using an AFM cantilever with a modified tip (attached glass sphere) (Figure 6a) with the same sample thickness (15 μm). The larger contact area of the glass probe increased the maximum adhesion force for all the three samples, whereas the corresponding displacements at the detachment were similar to those observed with the unmodified cantilever. The positions of the captured images are marked in Figure 6a. The first image of all three samples was identical, as observed with the unmodified cantilever. However, different diameters of the contact area were observed in the second image (Figure 6b,c,d). A slight decrease in adhesion force was also observed immediately after the acquisition of these images. The contact area of the CS sample [Figure 6b] gradually decreased during the release process, and the adhesion force decreased in response to the decreased volume of the elongated sample. The CL sample also exhibited a gradual decrease in the contact area with increasing adhesion force. These observations demonstrate that the CS and CL samples detached from the glass sphere because of the decreasing contact area prior to sufficient elongation of the sample despite good wettability of the contact surface. By contrast, the contact area of the PSA sample did not decrease drastically until detachment (Figure 6d) despite the thinner fibrillation at the beginning of the release process.

Images of the CL and PSA samples (thickness = 25 μm) were acquired at the same release velocity of 1.0 μm/s and compared (Figure 7a,b). The images were acquired with the glass sphere at the same height during the release process and just before detachment. The CL sample exhibited thicker fibrillation at the beginning of release, while the shrinkage of the contact area was visible throughout the release process until detachment. By contrast, the PSA sample maintained an almost constant contact area from the beginning. The fourth image was acquired at a height where the CL sample detached, exhibiting a necking of the fibrillation a few microns below the contact surface. As the sample further elongated, the necking became more prominent without rupture. Eventually, the contact area on the contact surface shrunk to a point to cause detachment. These observations proved that the prevention of shearing shrinkage of the contact area is essential for maximizing the adhesion performance, which can be achieved by adding a tackifier.

The adhesion force exceeded the load capacity of the AFM in both samples, whereas the adhesion force was independent of the sample thickness in the case of the unmodified

https://doi.org/10.1021/acs.langmuir.1c01381
Langmuir XXXX, XXX, XXX−XXX

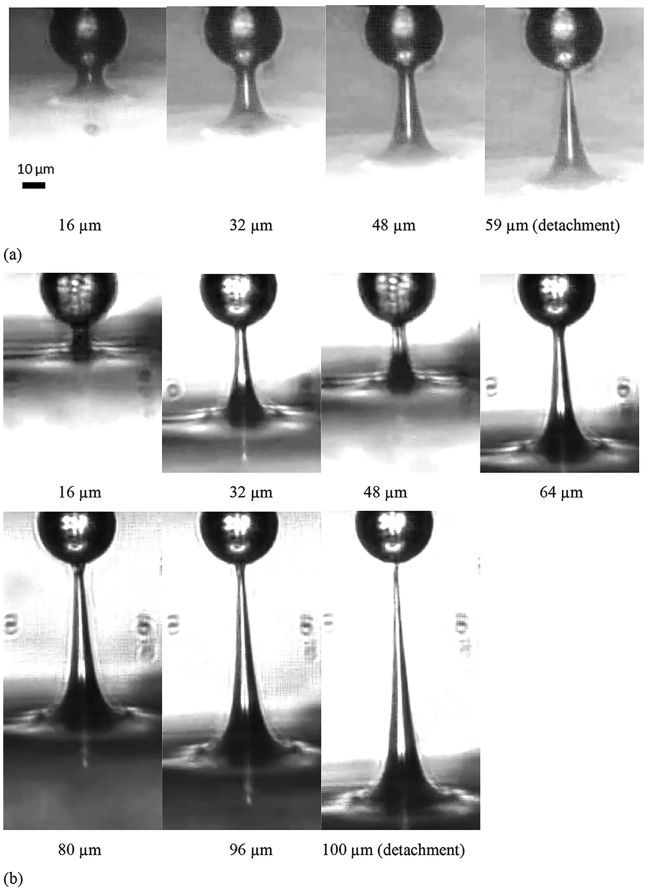

Figure 7. In situ observations of the release of an AFM cantilever with a release velocity of 1 μm/s (sample thickness = 25 μm) from the (a) CL and (b) PSA.

cantilever, as discussed earlier. This implies that the dependence of the maximum adhesion force on the sample thickness resulted from the difference in the probe shape. The angled contact surface of the unmodified cantilever led to a higher shearing force, particularly along the contact line, owing to the stress concentration (Figure 8a). Consequently, the contact area shrank to cause detachment. This detachment is independent of the sample thickness because localized high shear stress is generated along the contact outline. By contrast, the contact surface between the glass sphere and the sample surface was almost parallel; thus, the normal force was more dominant than the shearing force near the contact boundary. Assuming the normal force to be uniformly distributed throughout the contact area (Figure 8b), the corresponding normal stress is determined by the strain rate, which is the release velocity divided by the sample thickness. Our previous study using the same PSA sample also demonstrated that the adhesion forces at the detachment measured using a larger glass probe (diameter = 6.35 mm) were proportional to the contact area and determined by the strain rate after the gradual increase during the fibrillation, whereas those measured using an AFM cantilever were proportional to the contact radius.[31] However, the CS and CL samples still exhibited a decrease in the contact area because of insufficient stickiness to the glass sphere (Figure 8c). Similar sliding mechanics of a PSA sample without a tackifier was proposed for the detachment after cavity growth and expansion using a macroscopic probe tack test.[45]

Sticking Effect of the Tackifier during the Detachment Process. Although the acquired images clearly showed the elongation of the samples during the release process, it was still challenging to determine the nature of failure (adhesive or cohesive) that caused the detachment from the probe. The failure modes at detachment can be determined by repeated testing under the same conditions without cleaning the surface of the cantilever.[31] A detachment via cohesive failure would leave the probe surface covered with the fragmented sample, resulting in a significant reduction of the adhesion force after each successive test. By contrast, fully adhesive failure would provide reproducible results because the surface of the AFM cantilever remains pristine. In the present case, the ratio of the maximum forces measured in the second and the first test at corresponding release velocities (1−150 μm/s) was plotted (Figure 9). It can be inferred from the figure that the maximum force in the second test was significantly reduced at low release velocities. This reduction of the maximum force demonstrated that the fragmented PSA material was retained on the surface

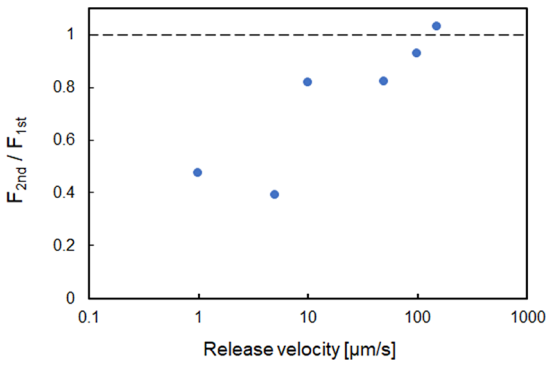

Figure 9. Relationship between the release velocity and the ratio of maximum adhesion forces for the first and second release tests.

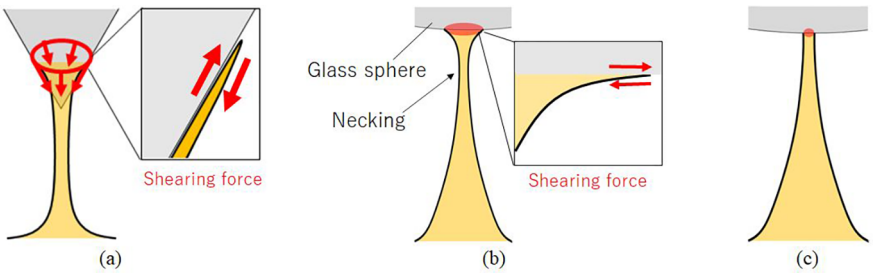

Figure 8. Local generation of a high strain rate along the contact outline because of shearing force in the case of the (a) AFM cantilever and the (b) AFM cantilever with an attached glass sphere, and (c) shrinkage of the contact area from the CL.

https://doi.org/10.1021/acs.langmuir.1c01381
Langmuir XXXX, XXX, XXX−XXX

of the cantilever because of the cohesive failure after the first test. At velocities ≥10 μm/s, the ratio increased dramatically to 0.8 and approached unity. At a release velocity of 150 μm/s, the ratio was higher than unity, indicating that the maximum force was higher in the second test. This suggests that the surface of the AFM cantilever became cleaner after the first test at higher velocities, and the failure mode transitioned from cohesive to adhesive. As the in situ observations of fibrillation in this study were conducted at a relatively low release velocity of 0.05 to 1.0 μm/s, the detachment observed in Figures 567 was attributed to the cohesive failure. In other words, the probe surface and the samples were strongly bonded, and the contact area was maintained until detachment.

As illustrated in Figure 8a, a very thin layer is formed along the contact outline of the cantilever because of high shear stress. As the sample continues to elongate, this layer becomes thinner so that the strain rate may increase drastically even under constant release velocity. The high storage and loss moduli of the PSA sample significantly increased the resistance against shearing deformation and prevented shrinkage of the contact area. Consequently, higher adhesion force was generated at a higher release velocity because of sufficient elongation of the inherent polymer network. The tackifier seemed to have less effect on the elongation of bulk fibrillation, as demonstrated by the DMA results (Figure 2a,b). A release velocity of 1 μm/s for the sample thickness 5−50 μm prepared in this study is equivalent to a strain rate of 0.02−0.2 s^{-1}. At such strain rates, both G' and G'' of the PSA sample were very similar to those of the CL sample. Hence, it was confirmed that the "sticking effect" of the tackifier on the contact area facilitated high resistance to the shearing shrinkage during release and enabled sufficient elongation of the sample at high release velocities.

CONCLUSIONS

This study investigated the adhesion mechanism of acrylic-based PSAs with a tackifier using DMA and in situ AFM analyses. The DMA results demonstrated that the addition of the tackifier significantly increased the storage and loss moduli at higher strain rates. These characteristics were corroborated by the AFM force measurements. Specifically, the maximum adhesion force at higher release velocities remained unaffected in the case of the copolymer solution and the cross-linked copolymer; however, it increased significantly when the tackifier was added. Furthermore, the in situ observations of the fibrillation process using a glass sphere revealed differences in the detachment process. In the case of the cross-linked polymer, the contact area gradually decreased as the fibrillation progressed. This was attributed to the shrinkage of the fibrils because of Poisson's effect, where the contact outline eventually shrunk to cause detachment. However, the final product with the tackifier maintained the contact area during elongation of the fibrils. The localized high storage and loss moduli generated by the shearing deformation led to necking just below the contact area because of resistance to the contact outline against shrinkage. The tackifier led to viscoelastic behavior of the PSA, which was essential for sticking to the contact area until sufficient elongation of the fibrils.

ASSOCIATED CONTENT

Supporting Information

The Supporting Information is available free of charge at https://pubs.acs.org/doi/10.1021/acs.langmuir.1c01381.

Chemical structure of the CS, which is composed of butyl acrylate, methyl methacrylate, and 4-hydroxybutyl acrylate (PDF)

AUTHOR INFORMATION

Corresponding Author

Kosuke Takahashi − *Division of Mechanical and Aerospace Engineering, Hokkaido University, Sapporo, Hokkaido 060-8628, Japan;* orcid.org/0000-0002-7399-3774; Email: ktakahashi@eng.hokudai.ac.jp

Authors

Futoshi Yanai − *Department of Transdisciplinary Science and Engineering, Tokyo Institute of Technology, Tokyo 152-8550, Japan*

Kazuaki Inaba − *Department of Transdisciplinary Science and Engineering, Tokyo Institute of Technology, Tokyo 152-8550, Japan*

Kikuo Kishimoto − *Department of Transdisciplinary Science and Engineering, Tokyo Institute of Technology, Tokyo 152-8550, Japan*

Yuichi Kozone − *LINTEC Corporation, Saitama 335-0005, Japan*

Toshio Sugizaki − *LINTEC Corporation, Saitama 335-0005, Japan*

Complete contact information is available at: https://pubs.acs.org/10.1021/acs.langmuir.1c01381

Author Contributions

The manuscript was written with the contributions of all authors. All the authors approved the final version of the manuscript.

Notes

The authors declare no competing financial interest.

REFERENCES

(1) Creton, C. Pressure-Sensitive Adhesives: An Introductory Course. *MRS Bull.* **2003**, *28*, 434−439.

(2) Webster, I. Recent Developments in Pressure-Sensitive Adhesives for Medical Applications. *Int. J. Adhes. Adhes.* **1997**, *17*, 69−73.

(3) Li, J.; Celiz, A. D.; Yang, J.; Yang, Q.; Wamala, I.; Whyte, W.; Seo, B. R.; Vasilyev, N. V.; Vlassak, J. J.; Suo, Z.; Mooney, D. J. Tough Adhesives for Diverse Wet Surfaces. *Science* **2017**, *357*, 378−381.

(4) Eveloy, V.; Rodgers, P.; Pecht, M. G. Reliability of Pressure-Sensitive Adhesive Tapes for Heat Sink Attachment in Air-Cooled Electronic Assemblies. *IEEE Trans. Device Mater. Reliab.* **2004**, *4*, 650−657.

(5) Lee, J. H.; Lee, T. H.; Shim, K. S.; Park, J. W.; Kim, H. J.; Kim, Y.; Jung, S. Effect of Crosslinking Density on Adhesion Performance and Flexibility Properties of Acrylic Pressure Sensitive Adhesives for Flexible Display Applications. *Int. J. Adhes. Adhes.* **2017**, *74*, 137−143.

(6) Chiche, A.; Pareige, P.; Creton, C. Role of Surface Roughness in Controlling the Adhesion of a Soft Adhesive on a Hard Surface. *Comptes Rendus l'Académie des Sci. - Ser. IV - Phys.* **2000**, *1*, 1197−1204.

(7) Lorenz, B.; Krick, B. A.; Mulakaluri, N.; Smolyakova, M.; Dieluweit, S.; Sawyer, W. G.; Persson, B. N. J. Adhesion: Role of Bulk Viscoelasticity and Surface Roughness. *J. Phys.: Condens. Matter* **2013**, *25*, No. 225004.

(8) Davis, C. S.; Lemoine, F.; Darnige, T.; Martina, D.; Creton, C.; Lindner, A. Debonding Mechanisms of Soft Materials at Short Contact Times. *Langmuir* **2014**, 10626.

(9) Creton, C.; Leibler, L. How Does Tack Depend on Time of Contact and Contact Pressure? *J. Polym. Sci., Part B: Polym. Phys.* **1996**, *34*, 545−554.
(10) Nakamura, Y.; Imamura, K.; Ito, K.; Nakano, S.; Sueoka, A.; Fujii, S.; Sasaki, M.; Urahama, Y. Contact Time and Temperature Dependencies of Tack in Polyacrylic Block Copolymer Pressure-Sensitive Adhesives Measured by the Probe Tack Test. *J. Adhes. Sci. Technol.* **2012**, *26*, 231−249.
(11) Villey, R.; Cortet, P. P.; Creton, C.; Ciccotti, M. In-Situ Measurement of the Large Strain Response of the Fibrillar Debonding Region during the Steady Peeling of Pressure Sensitive Adhesives. *Int. J. Fract.* **2017**, *204*, 175−190.
(12) Chopin, J.; Villey, R.; Yarusso, D.; Barthel, E.; Creton, C.; Ciccotti, M. Nonlinear Viscoelastic Modeling of Adhesive Failure for Polyacrylate Pressure-Sensitive Adhesives. *Macromolecules* **2018**, *51*, 8605−8610.
(13) Poivet, S.; Nallet, F.; Gay, C.; Teisseire, J.; Fabre, P. Force Response of a Viscous Liquid in a Probe-Tack Geometry: Fingering versus Cavitation. *Eur. Phys. J. E: Soft Matter Biol. Phys.* **2004**, *15*, 97−116.
(14) Ferguson, J.; Reilly, B.; Granville, N. Extensional and Adhesion Characteristics of a Pressure Sensitive Adhesive. *Polymer* **1997**, *38*, 795−800.
(15) Feldstein, M. M.; Siegel, R. A. Molecular and Nanoscale Factors Governing Pressure-Sensitive Adhesion Strength of Viscoelastic Polymers. *J. Polym. Sci., Part B: Polym. Phys.* **2012**, *50*, 739−772.
(16) Gdalin, B. E.; Bermesheva, E. V.; Shandryuk, G. A.; Feldstein, M. M. Effect of Temperature on Probe Tack Adhesion: Extension of the Dahlquist Criterion of Tack. *J. Adhes.* **2011**, *87*, 111−138.
(17) Gent, A. N.; Schultz, J. Effect of Wetting Liquids on the Strength of Adhesion of Viscoelastic Material. *J. Adhes.* **1972**, *3*, 281−294.
(18) Chang, E. P. Viscoelastic Windows of Pressure-Sensitive Adhesives. *J. Adhes.* **1991**, *34*, 189−200.
(19) Nakamura, Y.; Imamura, K.; Yamamura, K.; Fujii, S.; Urahama, Y. Influence of Crosslinking and Peeling Rate on Tack Properties of Polyacrylic Pressure-Sensitive Adhesives. *J. Adhes. Sci. Technol.* **2013**, *27*, 1951−1965.
(20) Ito, K.; Shitajima, K.; Karyu, N.; Fujii, S.; Nakamura, Y.; Urahama, Y. Influence of the Degree of Crosslinking on the Stringiness of Crosslinked Polyacrylic Pressure-Sensitive Adhesives. *J. Appl. Polym. Sci.* **2014**, *131*, 40336.
(21) Gurney, R.; Henry, A.; Schach, R.; Lindner, A.; Creton, C. Molecular Weight Dependence of Interdiffusion and Adhesion of Polymers at Short Contact Times. *Langmuir* **2017**, *33*, 1670−1678.
(22) Lindner, A.; Lestriez, B.; Mariot, S.; Creton, C.; Maevis, T.; Lühmann, B.; Brummer, R. Adhesive and Rheological Properties of Lightly Crosslinked Model Acrylic Networks. *J. Adhes.* **2006**, *82*, 267−310.
(23) Tobing, S.; Klein, A.; Sperling, L. H.; Petrasko, B. Effect of Network Morphology on Adhesive Performance in Emulsion Blends of Acrylic Pressure Sensitive Adhesives. *J. Appl. Polym. Sci.* **2001**, *81*, 2109−2117.
(24) Khan, I.; Poh, B. T. Natural Rubber-Based Pressure-Sensitive Adhesives: A Review. *J. Polym. Environ.* **2011**, *19*, 793−811.
(25) Lim, D. H.; Do, H. S.; Kim, H. J. PSA Performances and Viscoelastic Properties of SIS-Based PSA Blends with H-DCPD Tackifiers. *J. Appl. Polym. Sci.* **2006**, *102*, 2839−2846.
(26) Sasaki, M.; Fujita, K.; Adachi, M.; Fujii, S.; Nakamura, Y.; Urahama, Y. The Effect of Tackifier on Phase Structure and Peel Adhesion of a Triblock Copolymer Pressure-Sensitive Adhesive. *Int. J. Adhes. Adhes.* **2008**, *28*, 372−381.
(27) Tobing, S. D.; Klein, A. Mechanistic Studies in Tackified Acrylic Emulsion Pressure Sensitive Adhesives. *J. Appl. Polym. Sci.* **2000**, *76*, 1965−1976.
(28) Kim, H.-J.; Mizumachi, H. Miscibility and Peel Strength of Acrylic Pressure-sensitive Adhesives: Acrylic Copolymer−Tackifier Resin Systems. *J. Appl. Polym. Sci.* **1995**, *56*, 201−209.
(29) Takahashi, K.; Shimizu, M.; Inaba, K.; Kishimoto, K.; Inao, Y.; Sugizaki, T. Tack Performance of Pressure-Sensitive Adhesive Tapes under Tensile Loading. *Int. J. Adhes. Adhes.* **2013**, *45*, 90−97.
(30) Takahashi, K.; Yamagata, Y.; Inaba, K.; Kishimoto, K.; Tomioka, S.; Sugizaki, T. Characterization of Tack Strength Based on Cavity-Growth Criterion. *Langmuir* **2016**, *32*, 3525−3531.
(31) Takahashi, K.; Oda, R.; Inaba, K.; Kishimoto, K. Scaling Effect on the Detachment of Pressure-Sensitive Adhesives through Fibrillation Characterized by a Probe-Tack Test. *Soft Matter* **2020**, *16*, 6493−6500.
(32) Zosel, A. Adhesion and Tack of Polymers: Influence of Mechanical Properties and Surface Tensions. *Colloid Polym. Sci.* **1985**, *263*, 541−553.
(33) Zosel, A. Adhesive Failure and Deformation Behaviour of Polymers. *J. Adhes.* **1989**, *30*, 135−149.
(34) Lakrout, H.; Sergot, P.; Creton, C. Direct Observation of Cavitation and Fibrillation in a Probe Tack Experiment on Model Acrylic Pressure-Sensitive-Adhesives. *J. Adhes.* **1999**, *69*, 307−359.
(35) Yamaguchi, T.; Koike, K.; Doi, M. In Situ Observation of Stereoscopic Shapes of Cavities in Soft Adhesives. *Europhys. Lett.* **2007**, *77*, 64002.
(36) Zosel, A. The Effect of Fibrilation on the Tack of Pressure Sensitive Adhesives. *Int. J. Adhes. Adhes.* **1998**, *18*, 265−271.
(37) Yamaguchi, T.; Creton, C.; Doi, M. Simple Model on Debonding of Soft Adhesives. *Soft Matter* **2018**, *14*, 6206−6213.
(38) Creton, C.; Lakrout, H. Micromechanics of Flat-Probe Adhesion Tests of Soft Viscoelastic Polymer Films. *J. Polym. Sci., Part B: Polym. Phys.* **2000**, *38*, 965−979.
(39) Shull, K. R.; Creton, C. Deformation Behavior of Thin, Compliant Layers under Tensile Loading Conditions. *J. Polym. Sci., Part B: Polym. Phys.* **2004**, *42*, 4023−4043.
(40) Lin, Y. Y.; Hui, C.-Y.; Conway, H. D. A Detailed Elastic Analysis of the Flat Punch (Tack) Test for Pressure-Sensitive Adhesives. *J. Polym. Sci., Part B: Polym. Phys.* **2000**, *38*, 2769−2784.
(41) Jeusette, M.; Peeterbroeck, S.; Simal, F.; Cossement, D.; Roose, P.; Leclère, P.; Dubois, P.; Hecq, M.; Lazzaroni, R. Microscopic Morphology of Blends between a New "All-Acrylate" Radial Block Copolymer and a Rosin Ester Resin for Pressure Sensitive Adhesives. *Eur. Polym. J.* **2008**, *44*, 3931−3940.
(42) Nakamura, Y.; Sakai, Y.; Imamura, K.; Ito, K.; Fujii, S.; Urahama, Y. Effects of the Compatibility of a Polyacrylic Block Copolymer/Tackifier Blend on the Phase Structure and Tack of a Pressure-Sensitive Adhesive. *J. Appl. Polym. Sci.* **2012**, *123*, 2883−2893.
(43) Simal, F.; Jeusette, M.; Leclère, P.; Lazzaroni, R.; Roose, P. Adhesive Properties of a Radial Acrylic Block Co-Polymer with a Rosin Ester Resin. *J. Adhes. Sci. Technol.* **2012**, *21*, 559−574.
(44) Brown, K.; Hooker, J. C.; Creton, C. Micromechanisms of Tack of Soft Adhesives Based on Styrenic Block Copolymers. *Macromol. Mater. Eng.* **2002**, *287*, 163−179.
(45) Glassmaker, N. J.; Hui, C. Y.; Yamaguchi, T.; Creton, C. Detachment of Stretched Viscoelastic Fibrils. *Eur. Phys. J. E: Soft Matter Biol. Phys.* **2008**, *25*, 253−266.

https://doi.org/10.1021/acs.langmuir.1c01381
Langmuir XXXX, XXX, XXX−XXX